

This item is the archived peer-reviewed author-version of:

Joint reconstruction of attenuation, refraction and dark field X-ray phase contrasts using split Barzilai-Borwein steps

Reference:

Six Nathanaël, Renders Jens, De Beenhouwer Jan, Sijbers Jan.- Joint reconstruction of attenuation, refraction and dark field X-ray phase contrasts using split Barzilai-Borwein steps
Proceedings of the Society of Photo-optical Instrumentation Engineers / SPIE: International Society for Optical Engineering - ISSN 1996-756X - Bellingham, Spie-int soc optical engineering, 12242(2022), 1224200
Full text (Publisher's DOI): <https://doi.org/10.1117/12.2633587>
To cite this reference: <https://hdl.handle.net/10067/1944260151162165141>

Joint reconstruction of attenuation, refraction and dark field X-ray phase contrasts using split Barzilai-Borwein steps

Nathanaël Six^{a,b}, Jens Renders^{a,b}, Jan De Beenhouwer^{a,b}, and Jan Sijbers^{a,b,c}

^aimec-Vision Lab, Department of Physics, University of Antwerp, Belgium

^bDynXlab: Center for 4D Quantitative X-ray Imaging and Analysis, Antwerp, Belgium

^c μ NEURO Research Centre of Excellence, University of Antwerp, Antwerp, Belgium.

ABSTRACT

Edge illumination is a phase sensitive X-ray imaging technique, compatible with lab-based X-ray sources. Phase information can be retrieved by displacing two masks relative to each other with the object positioned in between. Phase retrieval then allows the three contrasts, absorption, refraction and dark field, to be individually reconstructed with FBP. In this work, a novel joint reconstruction method is proposed using a combined forward model, allowing the three contrasts to be reconstructed simultaneously, without a retrieval step. This allows for more freedom in the acquisition scheme. The proposed objective function is minimized using a split Barzilai-Borwein gradient method. Improved convergence speed and reconstruction quality on an experimental dataset, compared to existing methods, is shown.

Keywords: x-ray phase contrast, computed tomography, reconstructions, non-linear optimization

1. INTRODUCTION

X-ray phase contrast imaging (XPCI) techniques allow for the retrieval of complementary contrasts to the conventional X-ray attenuation contrast. These additional contrasts are comprised of a phase signal, related to the refraction of the X-ray beam and a scatter or dark-field signal, related to scattering due to sub-voxel microstructures.¹ These signals have been shown to generate a higher contrast in soft tissue compared to attenuation contrast and allow to visualize sub-voxel structures in, for example, composite materials.² Applications for XPCI have broadened from biomedical studies³⁻⁶ to non-destructive testing,⁷ materials science^{8,9} and security.^{10,11} Edge illumination (EI) is an emerging XPCI technique, well-suited for use with lab-based X-ray sources with a large focal spot and polychromatic spectrum.^{2,12} The phase information can be retrieved by displacing two strongly attenuating masks relative to each other with the object positioned in between. Traditionally, multiple images at a single view angle are taken, one for each mask displacement, after which a Gaussian is fitted to the data in each detector pixel. By comparing the Gaussians before and after the introduction of a sample, three complementary contrasts are retrieved: absorption, refraction and dark field. These separated contrasts are then reconstructed individually using for example FBP. As a result, the illumination curve at every detector pixel needs to be sampled adequately, resulting in long scan times, in case of computed tomography (CT). Furthermore, no information can be directly shared between the contrasts during reconstruction.

An alternative approach to the conventional two-step-approach, in which phase contrast images are reconstructed after phase retrieval, is a one-step-approach in which phase contrast images are directly reconstructed from the measured X-ray data. In this case, different contrasts are reconstructed simultaneously, without a retrieval step. In grating based Talbo-Lau interferometry (GBI), statistical approaches to one-step joint reconstruction have been proposed,^{13,14} where a likelihood function is minimized. These approaches were also shown to help reduce scan times as greater freedom in the scanning geometry is allowed.¹⁵ Unfortunately, these techniques cannot be directly used for EI setups, as the measurements of these modalities are different. GBI compares changes in an interference pattern while EI compares changes in illumination from macroscopic refraction. Therefore, forward models developed for GBI are not directly suited for EI data. Recently, a joint reconstruction method for EI, using gradient descent with line searches, was proposed for the reconstruction of

Send correspondence to nathanael.six@uantwerpen.be

the attenuation and phase contrasts.¹⁶ This method achieves a similar freedom in acquisition setup for EI as was reported in¹⁵ for GBI. However, the method in¹⁶ has the clear downside that the dark field contrast is no longer reconstructed. Furthermore, no investigation into different suitable solvers of the objective function was performed.

In this work, a novel joint reconstruction method is proposed using a combined Gaussian forward model, allowing all three contrasts to be reconstructed simultaneously. The resulting least-squares objective function is then minimized using gradient descent with split Barzilai-Borwein steps.¹⁷ We show reconstructions with the proposed method on an experimental dataset, comparing with phase retrieval and FBP reconstruction as well as line-search and classical Barzilai-Borwein gradient descent.

2. METHODS

2.1 Edge illumination CT forward model

In EI, the refraction of the X-rays in the object are measured by adding two gratings to the traditional X-ray setup, shown in Figure 1. The beam is split into smaller beamlets, one for each pixel on the detector, and can be partially blocked from reaching the detector by the detector mask. Moving the sample mask parallel to the detector mask, called phase stepping, changes the fraction of the beamlet that is blocked by the detector mask. The curve generated by measuring the intensities in function of these mask translation is called the illumination curve (IC), which is assumed to be approximately Gaussian. After the introduction of a sample, three contrasts can be retrieved by measuring the changes in the IC: attenuation, phase, and dark field. The change of area under the IC is a measure of the attenuation of the sample, the shift of the peak of the IC measures the refraction of the beamlet by the sample, and the broadening of the IC corresponds to the dark field signal.

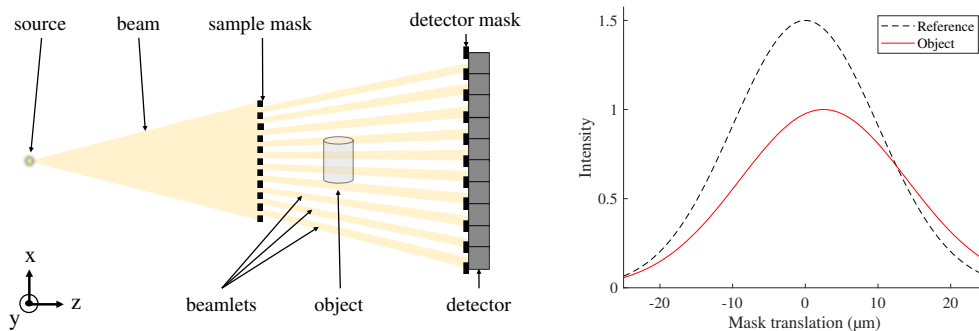


Figure 1. Left: overview of an EI setup. Right: flatfield and measured IC. Image courtesy of J. Sanctorum.

We denote the $n \times 1$ vectors corresponding to the attenuation, phase and dark field reconstruction as \mathbf{x}_μ , \mathbf{x}_δ , and \mathbf{x}_σ , respectively. These vectors can be combined in a single vector $\mathbf{x} \in \mathbb{R}^{3n}$. Furthermore, let $\mathbf{A} \in \mathbb{R}^{m \times n}$ be the discretised version of the Radon transform and $\mathbf{D} \in \mathbb{R}^{m \times m}$ the forward differences operator on vectors in \mathbb{R}^m . We assume a Gaussian model for the IC, such that the flatfield \mathbf{p}_0 can be modeled as:

$$\mathbf{p}_0(\xi) = a_0 \exp\left(-\frac{(\xi - b_0)^2}{2c_0^2}\right) + d_0, \quad (1)$$

with ξ the phase step and a_0, b_0, c_0, d_0 the parameters of the translated Gaussian: amplitude, mean, variance and offset, respectively. These parameters can be found by phase retrieval, i.e. fitting a Gaussian to the measured flatfield data. In this paper, we only do a single fit, on the mean flatfield. That is, only 4 parameters are fitted in the preprocessing step. We now consider the effects the introduction of the object \mathbf{x} has on the measurements. The attenuation of the object, with attenuation coefficients \mathbf{x}_μ , is modeled by the Beer-Lambert law in X-ray CT as:

$$\mathbf{I}(\mathbf{x}_\mu) = I_0 \exp(-\mathbf{A}\mathbf{x}_\mu), \quad (2)$$

with \mathbf{I} the measured intensity and I_0 the flatfield intensity. In the case of EI, the area under the IC is considered to decrease by attenuation, instead of the measured intensity. Therefore, we employ the same equation as Eq. 2, but with \mathbf{I} and I_0 understood to be areas under the measured and flatfield IC, respectively. Refraction of the object is based on the real part of the index of refraction. These values for the object are represented by \mathbf{x}_δ . As the beamlet is refracted, the mean of the measured IC shifts, with this shift given by:

$$\mathbf{s}(\mathbf{x}_\delta) = \mathbf{D}\mathbf{A}\mathbf{x}_\delta. \quad (3)$$

Lastly, the dark-field contrast models scattering in the object due to the presence of sub-voxel structures. This shows as broadening of the IC. We model this as the convolution of the IC with a normal distribution $\mathcal{N}(0, (\mathbf{A}\mathbf{x}_\sigma)^2)$. One then obtains the following joint forward projection model, where all operations with vectors are pointwise, except for the matrix-vector products with \mathbf{A} and \mathbf{D} :

$$\mathbf{p}(\mathbf{x}, \xi) = \exp(-\mathbf{A}\mathbf{x}_\mu) \left(\frac{a_0 c_0}{\sqrt{c_0^2 + (\mathbf{A}\mathbf{x}_\sigma)^2}} \exp\left(-\frac{(\xi - b_0 - \mathbf{D}\mathbf{A}\mathbf{x}_\delta)^2}{2(c_0^2 + (\mathbf{A}\mathbf{x}_\sigma)^2)}\right) + d_0 \right). \quad (4)$$

Analogously to the construction of \mathbf{x} , we can still represent \mathbf{p} as a vector when multiple phase steps ξ_i per projection angle are considered, by concatenating the different $\mathbf{p}(\mathbf{x}, \xi_i)$ to create a single vector, which we denote as $\mathbf{p}(\mathbf{x}, \boldsymbol{\xi})$.

2.2 Optimization

Given the forward model in Eq. 4 and some measured data \mathbf{b} , the reconstruction problem can be seen as a non-linear minimization problem of the following least-squares objective function:

$$\mathbf{f}(\mathbf{x}) = \frac{1}{2} \|\mathbf{p}(\mathbf{x}, \boldsymbol{\xi}) - \mathbf{b}\|_2^2. \quad (5)$$

With the reconstruction $\tilde{\mathbf{x}}$ being defined as:

$$\tilde{\mathbf{x}} = \operatorname{argmin}_{\mathbf{x}} \mathbf{f}(\mathbf{x}). \quad (6)$$

Gradient descent is a widespread iterative method for solving optimization problems of the form of Eq. 6, where the next iteration is found from the previous as:¹⁸

$$\mathbf{x}^{(k+1)} = \mathbf{x}^{(k)} - \alpha \nabla_{\mathbf{x}} \mathbf{f}|_{\mathbf{x}^{(k)}}. \quad (7)$$

The gradient $\nabla_{\mathbf{x}} \mathbf{f}$ can be seen as the concatenation of three gradients: $\nabla_{\mathbf{x}} \mathbf{f} = [\nabla_{\mathbf{x}_\mu} \mathbf{f}^\top \quad \nabla_{\mathbf{x}_\delta} \mathbf{f}^\top \quad \nabla_{\mathbf{x}_\sigma} \mathbf{f}^\top]^\top$. Defining $\mathbf{r}(\mathbf{x}) = \mathbf{p}(\mathbf{x}, \boldsymbol{\xi}) - \mathbf{b}$, one can calculate these gradients to be equal to the following, in the case of a single phase step per projection angle:

$$\begin{aligned} \nabla_{\mathbf{x}_\mu} \mathbf{f} &= -\mathbf{A}^\top (\mathbf{p}(\mathbf{x}, \boldsymbol{\xi}) \mathbf{r}(\mathbf{x})) \\ \nabla_{\mathbf{x}_\delta} \mathbf{f} &= \mathbf{A}^\top \mathbf{D}^\top \left(\left(\frac{\xi - b_0 - \mathbf{D}\mathbf{A}\mathbf{x}_\delta}{c_0^2 + (\mathbf{A}\mathbf{x}_\sigma)^2} \right) (\mathbf{p}(\mathbf{x}, \boldsymbol{\xi}) - d_0 \exp(-\mathbf{A}\mathbf{x}_\mu)) \mathbf{r}(\mathbf{x}) \right) \\ \nabla_{\mathbf{x}_\sigma} \mathbf{f} &= \mathbf{A}^\top \left(\left(\frac{\mathbf{A}\mathbf{x}_\sigma}{c_0^2 + (\mathbf{A}\mathbf{x}_\sigma)^2} \right) \left(\frac{(\xi - b_0 - \mathbf{D}\mathbf{A}\mathbf{x}_\delta)^2}{c_0^2 + (\mathbf{A}\mathbf{x}_\sigma)^2} - 1 \right) (\mathbf{p}(\mathbf{x}, \boldsymbol{\xi}) - d_0 \exp(-\mathbf{A}\mathbf{x}_\mu)) \mathbf{r}(\mathbf{x}) \right), \end{aligned} \quad (8)$$

with all operations between vectors being executed pointwise. If multiple phase steps per projection angle would be taken, the resulting gradient is the sum of the gradients of the form described in Eq. 8 at each of the phase steps. For finding a suitable value of α in Eq. 7 multiple options exist.¹⁸ In this paper we will be considering two options. First, a line search based on Armijo conditions, as proposed for a two contrast method in.¹⁶ Secondly, the Barzilai-Borwein scheme¹⁷ which calculates the step size in iteration k as:

$$\alpha = \frac{(\mathbf{x}^{(k)} - \mathbf{x}^{(k-1)}) \cdot (\nabla_{\mathbf{x}} \mathbf{f}|_{\mathbf{x}^{(k)}} - \nabla_{\mathbf{x}} \mathbf{f}|_{\mathbf{x}^{(k-1)}})}{(\nabla_{\mathbf{x}} \mathbf{f}|_{\mathbf{x}^{(k)}} - \nabla_{\mathbf{x}} \mathbf{f}|_{\mathbf{x}^{(k-1)}}) \cdot (\nabla_{\mathbf{x}} \mathbf{f}|_{\mathbf{x}^{(k)}} - \nabla_{\mathbf{x}} \mathbf{f}|_{\mathbf{x}^{(k-1)}})}. \quad (9)$$

In addition to using these methods to find a single step size α , we also consider a split method where three separate step sizes $\alpha_1, \alpha_2, \alpha_3$ are calculated for the partial gradients shown in Eq. 8. One advantage of the proposed approach is that in contrast to the conventional two step method of reconstructing after phase retrieval, solving Eq. 6 does not require each pixel in each projection to have a fully sampled IC. This was also shown in¹⁶ for two contrasts. A benefit of using gradient descent is that box constraints can be added trivially by projecting after each iteration. For both \mathbf{x}_μ and \mathbf{x}_δ , non-negativity constraints, which are a type of box constraint, are a logical choice as negative values in the index of refraction would be physically impossible.

All multiplications with the system matrix \mathbf{A} or its transposed are performed on the GPU using the ASTRA toolbox.¹⁹

3. EXPERIMENTS & RESULTS

To evaluate the performance of the proposed joint reconstruction method, reconstructions of an experimental dataset were compared. The considered dataset was the central slice of a cone beam edge illumination dataset, acquired at the Advanced X-Ray Imaging Group of prof. A. Olivo, University College London. The imaged object was a fiber polymer block with woven fibers in two directions, held in place by plastic straws. A total number of 1250 projections were acquired over a 360° range, with 5 phase steps per projection angle. From this fully sampled dataset, images were reconstructed using the conventional two step method, first retrieving the different contrasts in each pixel and then reconstructing using FBP with a Ram-Lak filter, for attenuation and dark-field, or a Hilbert filter, for refraction. The reconstructions are shown in the first row of Figure 2.

Next, the same dataset was reconstructed with the proposed joint reconstruction method, with non-negativity constraints imposed on \mathbf{x}_μ and \mathbf{x}_δ . Both Armijo line search and Barzilai-Borwein methods for finding a suitable step size α were tested. We tested both single step size and the split approach, one step size for each partial gradient. For each iteration, the computation time was measured and the objective function, which is the 2-norm of the projection error, was calculated. All methods were run for 200 iterations.

A comparison of the methods from these measures is shown in the left plot in Figure 3. This plot clearly shows that the split BB method converges faster and to a lower error. The split Armijo line search method failed to find a suitable step size after 9 iterations, and therefore stops first in the plot. The reconstructions of the joint reconstruction method with split BB steps are shown in the second row of Figure 2. The reconstructions with the joint reconstruction method are largely comparable to the reconstructions after phase retrieval. The attenuation reconstructions are very similar. The contrast in the refraction and dark field reconstructions is higher for the joint reconstruction method. However, the streaking artefact in the dark field, present in both reconstructions due to directionality of the scatter, is also more pronounced in the reconstructions from the joint method.

Lastly, a subset of the fully sampled dataset was taken, where only one phase step was considered per projection. Thus, for this subset, the size of the projection data was the same as a conventional X-ray CT scan. The chosen phase step changes at each projection angle, so after five projection angles all five available phase steps have been sampled once. This dataset was also reconstructed using the proposed method and compared to the reconstructions of the full dataset. Note that this undersampled dataset cannot be reconstructed using the conventional two step method, as no reasonable Gaussian fitting is possible to a single point. Again, four options for calculating the step size are tested. A comparison of the methods is shown in the right plot in Figure 3. As in the previous case, the split BB method converges faster and to a lower error. The reconstructions of the joint reconstruction method with split BB steps on the subsampled dataset are shown in the third row of Figure 2. These reconstructions show more artefacts than the previous ones, which is to be expected as the amount of available data was reduced by a factor of five. The dark field image in particular shows many streaks outside of the sample. However, key features of the sample are still reconstructed well in all three contrasts.

4. DISCUSSION & CONCLUSION

The standard CT reconstruction method for EI involves a two step procedure of first fitting Gaussian functions to the IC of each pixel and subsequently reconstructing three contrasts separately with FBP. A main drawback of this method is the need for full sampling of each of these ICs at every projection angle. A recently proposed joint reconstruction method for single shot EI resolves this drawback by minimizing a combined forward model for

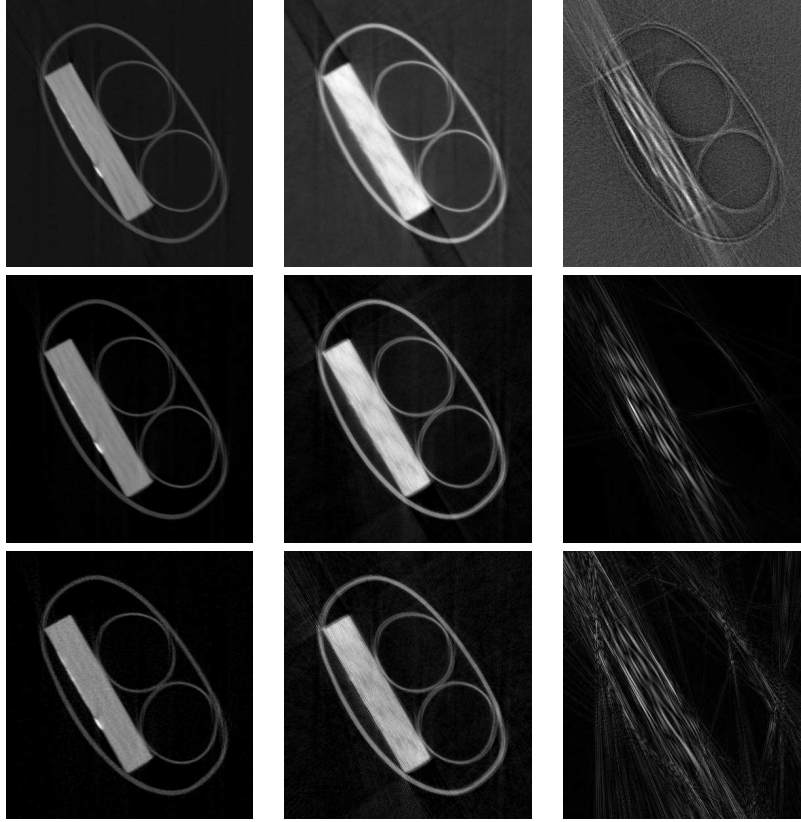


Figure 2. Reconstructions of the fiber polymer block. Columns from left to right: attenuation, refraction, and dark field. Rows from top to bottom: reconstruction after phase retrieval, joint reconstruction method on full dataset, joint reconstruction method on subset of the data with only one phase step per projection.

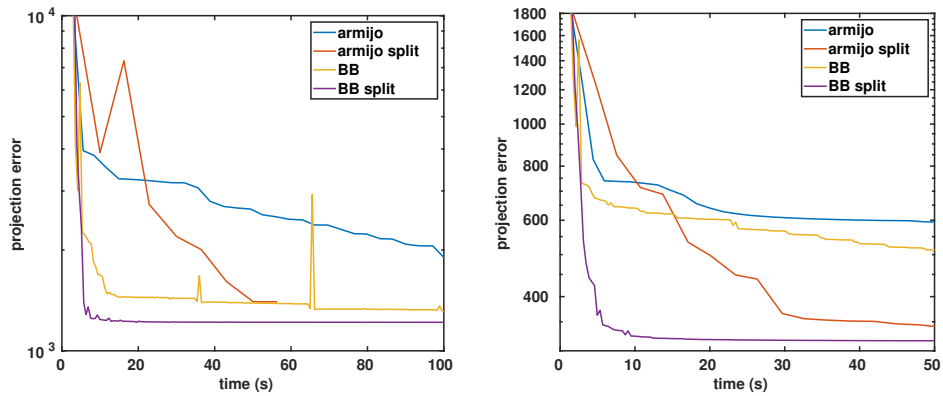


Figure 3. Plots of the projection error over time for the different methods to choose the step size, for the full dataset (left) and the subset of the data (right).

attenuation and refraction, using gradient descent with a line search. In this paper, we presented a joint reconstruction method that reconstructs all three contrasts: attenuation, refraction, and dark field. We furthermore investigated different step size choices in gradient descent and conclude that the use of a split Barzilai-Borwein scheme performed better than the standard Barzilai-Borwein scheme or Armijo line searches in terms of convergence speed and reconstruction quality. Future work includes the study of the performance of other quasi-Newton methods on the proposed objective function and the addition of regularization terms. Additionally, the forward

model proposed here can also be used as the model for iterative statistical reconstruction methods, by adjusting the objective function according to a chosen noise model.

ACKNOWLEDGMENTS

Nathanaël Six and Jens Renders have PhD fellowships of the FWO, (11D8319N) and (1SA2920N), respectively. This research was also supported by EU Interreg Flanders - Netherlands Smart*Light (0386), and the Research Foundation - Flanders (G090020N, G094320N, S003421N).

REFERENCES

- [1] Endrizzi, M., “X-ray phase-contrast imaging,” *Nuclear Instruments & Methods in Physics Research A* **878**, 88–98 (JAN 11 2018).
- [2] Olivo, A., “Edge-illumination X-ray phase-contrast imaging,” *Journal of Physics: Condensed Matter* **33**, 363002 (sep 2021).
- [3] Momose, A., Takeda, T., Itai, Y., and Hirano, K., “Phase-contrast X-ray computed tomography for observing biological soft tissues,” *Nature medicine* **2**(4), 473–475 (1996).
- [4] Arfelli, F., Assante, M., Bonvicini, V., et al., “Low-dose phase contrast X-ray medical imaging,” *Physics in Medicine & Biology* **43**(10), 2845 (1998).
- [5] Marenzana, M., Hagen, C. K., Borges, P. D. N., et al., “Synchrotron-and laboratory-based X-ray phase-contrast imaging for imaging mouse articular cartilage in the absence of radiopaque contrast agents,” *Philosophical Transactions of the Royal Society A: Mathematical, Physical and Engineering Sciences* **372**(2010), 20130127 (2014).
- [6] Massimi, L., Suaris, T., Hagen, C. K., et al., “Volumetric High-Resolution X-Ray Phase-Contrast Virtual Histology of Breast Specimens With a Compact Laboratory System,” *IEEE Transactions on Medical Imaging* **41**, 1188–1195 (may 2022).
- [7] Shoukroun, D., Massimi, L., Endrizzi, M., et al., “Edge illumination X-ray phase contrast imaging for impact damage detection in CFRP,” *Materials Today Communications* **31**, 103279 (jun 2022).
- [8] Hu, Z., Thomas, P., Snigirev, A., et al., “Phase-mapping of periodically domain-inverted LiNbO₃ with coherent X-rays,” *Nature* **392**(6677), 690–693 (1998).
- [9] Revol, V., Jerjen, I., Kottler, C., et al., “Sub-pixel porosity revealed by X-ray scatter dark field imaging,” *Journal of Applied Physics* **110**(4), 044912 (2011).
- [10] Olivo, A., Chana, D., and Speller, R., “A preliminary investigation of the potential of phase contrast X-ray imaging in the field of homeland security,” *Journal of Physics D: Applied Physics* **41**(22), 225503 (2008).
- [11] Olivo, A., Ignatyev, K., Munro, P., and Speller, R., “Design and realization of a coded-aperture based X-ray phase contrast imaging for homeland security applications,” *Nuclear Instruments and Methods in Physics Research A* **610**, 604–614 (nov 2009).
- [12] Zamir, A., Hagen, C., Diemoz, P. C., et al., “Recent advances in edge illumination X-ray phase-contrast tomography,” *Journal of Medical Imaging* **4**, 1 (oct 2017).
- [13] Ritter, A., Bayer, F., Durst, J., et al., “Simultaneous maximum-likelihood reconstruction for x-ray grating based phase-contrast tomography avoiding intermediate phase retrieval,” *arXiv preprint arXiv:1307.7912* (2013).
- [14] Brendel, B., von Teuffenbach, M., Noël, P. B., et al., “Penalized maximum likelihood reconstruction for x-ray differential phase-contrast tomography,” *Medical physics* **43**(1), 188–194 (2016).
- [15] Teuffenbach, M. v., Koehler, T., Fehringer, A., et al., “Grating-based phase-contrast and dark-field computed tomography: a single-shot method,” *Scientific reports* **7**(1), 1–8 (2017).
- [16] Chen, Y., Guan, H., Hagen, C. K., et al., “Single-shot edge illumination X-ray phase-contrast tomography enabled by joint image reconstruction,” *Optics Letters* **42**(3), 619–622 (2017).
- [17] Barzilai, J. and Borwein, J. M., “Two-point step size gradient methods,” *IMA journal of numerical analysis* **8**(1), 141–148 (1988).
- [18] Nocedal, J. and Wright, S. J., [*Numerical Optimization*], Springer, New York, NY, USA, 2e ed. (2006).
- [19] van Aarle, W., Palenstijn, W. J., Cant, J., et al., “Fast and flexible X-ray tomography using the ASTRA toolbox,” *Optics Express* **24**(22), 25129–25147 (2016).